Studies of the Anodic Oxidation of 1,4-Diazabicyclo[2.2.2]octane. Reactions of the Radical Cation

Zi-Rong Zheng,[†] Dennis H. Evans,*[,†] and Stephen F. Nelsen[‡]

The Department of Chemistry and Biochemistry, University of Delaware, Newark, Delaware 19716, and the Department of Chemistry, University of Wisconsin, Madison, Wisconsin 53706-1396

Received November 2, 1999

The title compound (**1**) was studied at platinum and gold electrodes in acetonitrile. A reversible oxidation peak occurs at +0.30 V vs the standard potential for ferrocenium ion/ferrocene. This process is followed by a second irreversible anodic peak that is due to the oxidation of the initially formed radical cation to the dication. The principal ultimate product of the first oxidation, the conjugate acid of **1**, is also oxidized over the range of potentials corresponding to the second anodic peak. The rate of disappearance of the radical cation of **1** has been determined by cyclic voltammetry. The results are best interpreted in terms of parallel pseudo-first-order decay ($k_1 = 0.6\ s^{-1}$) and second-order reactions. The first of these second-order reactions is either proton transfer from the radical cation to neutral **1** or hydrogen atom abstraction by the radical cation from neutral **1**, reactions that give the same products ($k_2 = 100\ M^{-1}\ s^{-1}$) and are kinetically indistinguishable. The other second-order reaction is the hydrogen-atom-transfer disproportionation of the radical cation giving the conjugate acid of **1** and the immonium ion ($k_3 = 100\ M^{-1}\ s^{-1}$). Both second-order processes must be included to account for the results. The present results are thought to be the first experimental evidence for the occurrence of hydrogen-atom-transfer disproportionation of amine radical cations.

Introduction

1,4-Diazabicyclo[2.2.2]octane, **1**, was the first tertiary diamine that was shown to have a relatively stable radical cation, $\mathbf{1}^{+\bullet}$, that could be detected by cyclic voltammetry and room-temperature electron spin resonance.[1] The unusual stability of the radical cation was attributed to through-space interaction of nitrogen orbitals, which leads to the positive charge being delocalized over both nitrogen atoms.[2] However, Hoffmann and coworkers pointed out that $\mathbf{1}^{+\bullet}$ is an excellent example of through-bond coupling, predicting on the basis of calculations that its singly occupied molecular orbital is not the antisymmetric lone pair combination the predominant through-space interaction requires, but instead is symmetric, predominately the combination of lone pair and σ(CC) bonds indicated diagrammatically on the structure shown.[3] Heilbronner and Muszkat showed that Hoffmann's assignment is correct using photoelectron spectroscopy.[4]

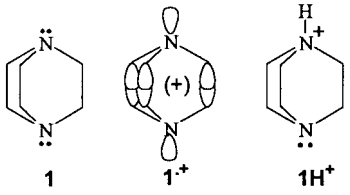

Early investigations of the anodic oxidation of tertiary amines include those of Dapo and Mann[5] as well as Russell,[6] who found the protonated amine as the main product. It was proposed that the initially formed radical cation of the tertiary amine abstracted a hydrogen atom from solvent to give the protonated amine and solvent radicals that underwent further reactions. In a later study of the oxidation of tripropylamine, Smith and Mann[7] showed that propanal was formed in addition to the protonated amine and explained the result by the reactions in Scheme 1. The initially formed radical cation was thought to lose a proton to the strongest base present in the system, the unreacted tertiary amine. In fact, as pointed out by Nelsen and Ippoliti,[2] it was long thought that the radical cations of tertiary amines are very strong acids, but this is not generally so as shown by the pK_a value of 8 in water determined for the radical cation of trimethylamine.[8a] (Nelsen and Ippoliti[2] calculated a value

Scheme 1

$$Pr_2\ddot{N}CH_2CH_2CH_3 \rightleftharpoons Pr_2\overset{+\cdot}{N}CH_2CH_2CH_3 + e^-$$

$$Pr_2\overset{+\cdot}{N}CH_2CH_2CH_3 + Pr_2\ddot{N}CH_2CH_2CH_3 \longrightarrow Pr_2\ddot{N}\dot{C}HCH_2CH_3 + Pr_3NH^+$$

$$Pr_2\ddot{N}\dot{C}HCH_2CH_3 \rightleftharpoons Pr_2\overset{+}{N}{=}CHCH_2CH_3 + e^-$$

$$2\ Pr_2\ddot{N}\dot{C}HCH_2CH_3 \longrightarrow Pr_2\ddot{N}CH_2CH_2CH_3 + Pr_2\ddot{N}CH{=}CHCH_3$$

$$Pr_2\overset{+}{N}{=}CHCH_2CH_3 + H_2O \longrightarrow Pr_2NH_2^+ + CH_3CH_2CHO$$

$$Pr_2\ddot{N}CH{=}CHCH_3 + H_2O \longrightarrow Pr_2NH + CH_3CH_2CHO$$

[†] University of Delaware.
[‡] University off Wisconsin.

(1) McKinney, T. M.; Geske, D. H. *J. Am. Chem. Soc.* **1965**, *87*, 3013−3014.
(2) Nelsen, S. F.; Ippoliti, J. T. *J. Am. Chem. Soc.* **1986**, *108*, 4879−4881.
(3) (a) Hoffmann, R.; Imamura, A.; Hehre, W. J. *J. Am. Chem. Soc.* **1968**, *90*, 1499−1509. (b) Hoffmann, R. *Acc. Chem. Res.* **1971**, *4*, 1−9.
(4) Heilbronner, E.; Muszkat, K. A. *J. Am. Chem. Soc.* **1970**, *92*, 3818−3820.
(5) Dapo, R. F.; Mann, C. K. *Anal. Chem.* **1963**, *35*, 677−680.
(6) Russell, C. D. *Anal. Chem.* **1963**, *35*, 1291−1292.

10.1021/jo991709v CCC: $19.00
Published on Web 02/25/2000

Scheme 2

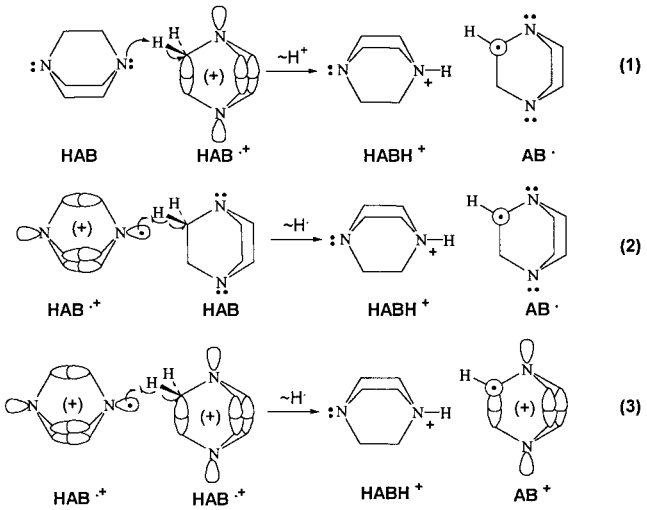

of 15 for the pK_a of the tertiary amine 9-(2-adamantyl)-9-azabicyclo[3.3.1]nonane but, as was pointed out later,[8b] this value is too high owing to a numerical error. However, in view of the experimental value for trimethylamine,[8a] the error is probably not as large as the 10 pK_a units that was claimed.[8b]) Hydrogen atom abstraction from the tertiary amine by the radical cation, a process that gives the same products as proton transfer, might very well be the preferred reaction (compare reactions 1 and 2, Scheme 2).

An even more favorable reaction would be the hydrogen-atom-transfer disproportionation of the radical cations (reaction 3), and Nelsen and Ippoliti speculated that this may be the most important decay route for the radical cations formed upon anodic oxidation of tertiary amines because their concentration will be high near the electrode surface, thus favoring this second-order reaction.[2a]

The relatively long lifetime of the radical cation of **1** affords the opportunity for rather straightforward electrochemical measurements of its rate of decay and a means of distinguishing among the mechanistic possibilities outlined above.

Results

Presented in Figure 1 is a typical voltammogram for **1** obtained with a platinum electrode in acetonitrile containing 0.10 M Bu_4NClO_4. The first oxidation peak occurs near +0.3 V vs the ferrocenium ion/ferrocene standard potential, a potential that will serve as reference for all results reported in this paper. The process responsible for this peak is the aforementioned oxidation of **1** to the radical cation. At more positive potentials there appears a second oxidation peak that is unusually drawn out along the potential axis. In fact, if treated as a simple irreversible electron-transfer process, the shape of the peak corresponds to a transfer coefficient of about 0.20. At least two species are responsible for this second oxidation. The first is the radical cation of **1**, which is presumably being oxidized to the dication, and the second is protonated **1** (**1**-H^+), which coincidentally is oxidized over the same range of potentials.

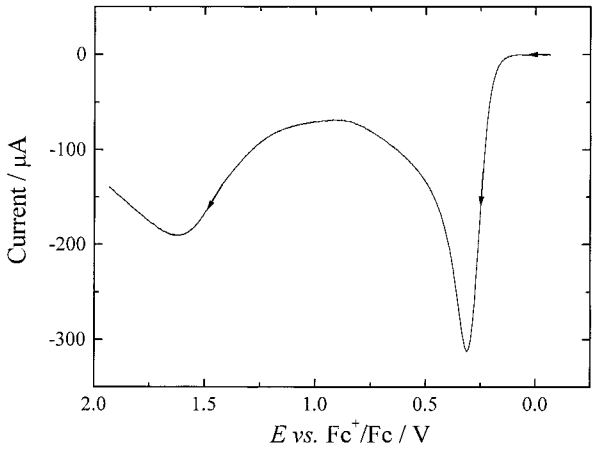

Figure 1. Cyclic voltammogram of 5.0 mM 1,4-diazabicyclo-[2.2.2]octane, **1**, at 0.50 V/s with a platinum disk working electrode. Electrolyte: 0.10 M Bu_4NClO_4 in acetonitrile.

Protonated **1** is formed by the follow-up reactions of the radical cation, and its presence is also signaled by a broad reduction peak seen at low scan rates around −1.4 V on the negative-going sweep after changing the scan direction at +0.5 V. When **1**-H^+ is formed in situ by titration of **1** with methanesulfonic acid, the height of the oxidation peak for **1** at +0.3 V decreased linearly with the amount of acid added leaving only the broad oxidation peak for **1**-H^+ at about +1.6 V while the reduction peak for **1**-H^+ at −1.4 V increased linearly with the amount of acid added. The cathodic reaction is the reduction of **1**-H^+ to dihydrogen and free base.

Controlled potential electrolysis of a solution of **1** at a potential positive of the first oxidation peak resulted in passage of typically 0.8 faradays per mole of **1** with isolation of the hydroperchlorate, **1**·$HClO_4$, in about 70% yield. We were not successful in identifying other products.

Similar electrolyses of **1** at potentials on the broad, irreversible second oxidation peak were plagued by the deposit of an insulating film on the electrode surface. It is known that treatment of **1** in water with the strong oxidant perchloryl fluoride results in oxidative ring opening and hydrolysis giving piperazine and formaldehyde, which subsequently polymerize.[9] Possibly similar polymerization reactions are responsible for the electrode passivation seen here.

We return now to the primary oxidation of **1** that produces the peak near +0.3 V. The potential range in the voltammograms in Figures 2−4 is restricted to include only the peak for oxidation to the radical cation and its subsequent reduction to starting material. Over the range of scan rates and concentrations investigated, the voltammograms have cathodic peak currents that are almost as large as expected if the radical cation were stable, at low concentrations and high scan rates, while at high concentrations and low scan rates considerable loss of radical cation is noted. This concentration dependence suggests that second-order reactions are involved in the decomposition of the radical cation of **1**.

Included in Figures 2−4 are digital simulations that have been fit to the experimental data considering three possible reactions: (1) pseudo-first-order hydrogen atom

(7) Smith, P. J.; Mann, C. K. *J. Org. Chem.* **1969**, *34*, 1821−1826.
(8) (a) Das, S.; von Sonntag, C. *Z. Naturforsch., B: Chem. Sci.* **1986**, *41B*, 505−513. (b) Dinnocenzo, J. P.; Banach, T. E. *J. Am. Chem. Soc.* **1989**, *111*, 8646−8653.

(9) Gardner, D. M.; Helitzer, R.; Rosenblatt, D. H. *J. Org. Chem.* **1967**, *32*, 1115−1119.

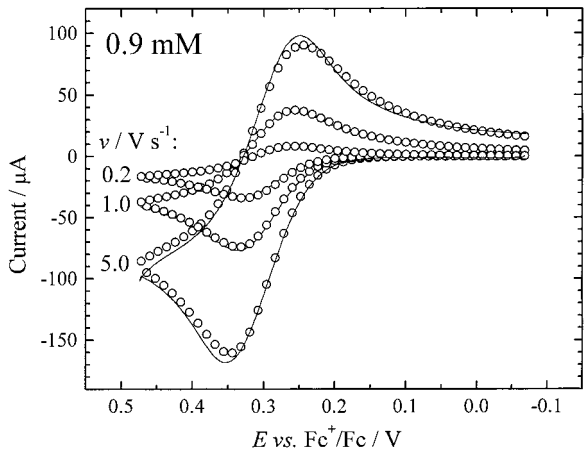

Figure 2. Cyclic voltammograms (full curves) of 0.9 mM **1** at 0.2, 1, and 5 V/s with a gold disk working electrode. Other conditions as in Figure 1. Symbols: Digital simulations with $E^{\circ}_{HAB^+/HAB} = 0.30$ V, $k_{s,HAB^+/HAB} = 0.05$ cm/s, $\alpha_{HAB^+/HAB} = 0.4$, $E^{\circ}_{AB^+/AB} = -0.6$ V, $k_{s,AB^+/AB} = 10^4$ cm/s, $\alpha_{AB^+/AB} = 0.5$, $k_1 = 0.6$ s^{-1}, $k_2 = k_3 = 100$ M^{-1} s^{-1} k_s and α are the standard heterogeneous electron-transfer rate constant and transfer coefficient of the indicated reactions. The chemical reactions are regarded as irreversible, and it is considered that once formed **AB**• is rapidly oxidized by **HAB**+• or the electrode. All diffusion coefficients were 2.1×10^{-5} cm^2/s. The electrode area was 0.071 cm^2 and no solution resistance was included in the simulation.

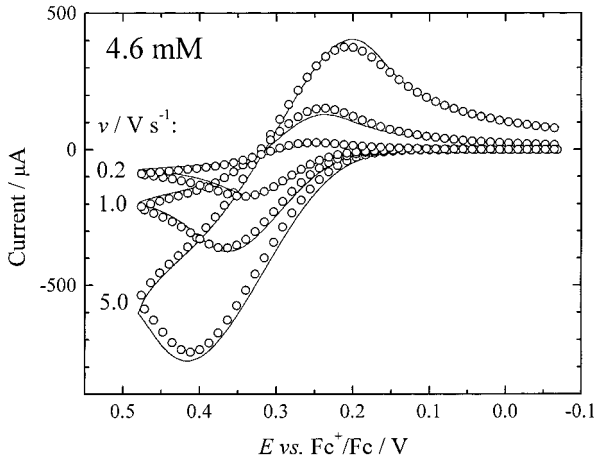

Figure 3. Cyclic voltammograms (full curves) of 4.6 mM **1** at 0.2, 1, and 5 V/s with a gold disk working electrode. Symbols: Digital simulations with same parameters as in Figure 2 except that 70 Ω of solution resistance was used in the simulation.

abstraction from the surroundings with rate constant k_1;[10] (2) proton transfer/hydrogen atom abstraction reactions 1 and 2 (which cannot be kinetically distinguished) with rate constant k_2; (3) hydrogen-atom-transfer dis-

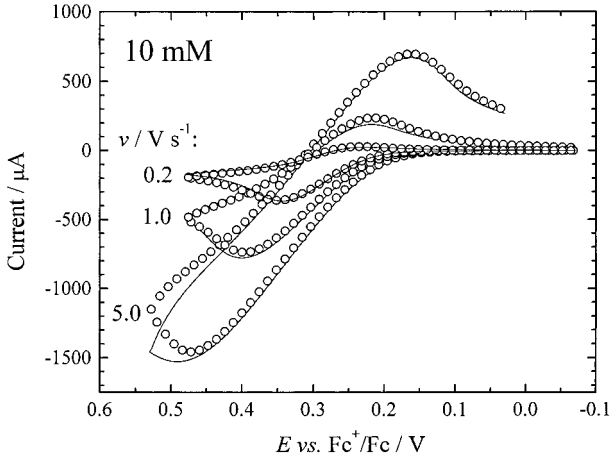

Figure 4. Cyclic voltammograms (full curves) of 10 mM **1** at 0.2, 1, and 5 V/s with a gold disk working electrode. Symbols: Digital simulations with same parameters as in Figure 2 except that 80 Ω of solution resistance was used in the simulation and $E^{\circ}_{HAB^+/HAB} = 0.29$ V.

proportionation reaction 3 with rate constant k_3. The concentration dependence mentioned above signals the impossibility of accounting for the results with only the first-order process 1. It proved to be possible to obtain relatively good fits with a combination of reaction 1 and either of the second-order processes, reaction 2 or 3. As will be shown later, a separate set of experiments shows that the best agreement is found when both reactions 2 and 3 are considered to contribute to the decay of the radical cation. The simulations shown in Figures 2−4 are taken from a total of 18 experiments at scan rates from 0.1 to 5 V/s and concentrations of 0.9, 4.6, and 10 mM. The rate constants giving best agreement between simulation and experiment were $k_1 = 0.6$ s^{-1} and $k_2 = k_3 = 100$ M^{-1} s^{-1}.

In complex electrochemical reaction mechanisms it is generally difficult to distinguish between two schemes with second-order reactions even though the reactants are quite different. In reactions 1 and 2, the radical cation being generated at the anode reacts with starting material that it encounters as it diffuses from the electrode surface. In reaction 3, the radical cation reacts with itself. The following experimental strategy is useful in providing a distinction: voltammetric experiments are carried out in which the switching potential is varied progressively from values near the foot of the anodic peak to values close to the peak. When the switching potential is near the foot, the concentration of radical cations produced will be only a small fraction of the bulk concentration of reactant **1**. Under these conditions, disproportionation reaction 3 will not be favored but reactions 1 and 2 will proceed at a substantial rate because the concentration of **1** at the surface has hardly been lowered from the bulk value. Conversely, at switching potentials near the peak, the surface concentration of the radical cation is large and approaches the bulk concentration of **1** favoring disproportionation whereas reactions 1 and 2 are impeded by the relatively low concentration of **1** at the surface due to its depletion by the electrolysis. This strategy is an adaptation of an earlier scheme developed and applied with the technique of chronopotentiometry.[11]

(10) (a) An alternative first-order reaction of the radical cation, C−C cleavage, has been mentioned in the literature.[9,10b−d] The ring-opened product, a distal radical cation, should be immediately oxidized to the dication, which would give piperazine and formaldehyde by hydrolysis during workup. The fact that 70% of the reactant is recovered as **1**·$HClO_4$ and that the second-order reactions to be discussed account for part of the missing 30% suggest that such C−C cleavage at the level of the radical cation cannot be very important. (b) Dennis, W. H.; Hull, L. A.; Rosenblatt, D. H. *J. Org. Chem.* **1967**, *32*, 3783−3787. (c) Hull, L. A.; Giordano, W. P.; Rosenblatt, D. H.; Davis, G. T.; Mann, C. K.; Milliken, S. B. *J. Phys. Chem.* **1969**, *73*, 2147−2152. (d) Davis, G. T.; Demek, M. M.; Rosenblatt, D. H. *J. Am. Chem. Soc.* **1972**, *94*, 3321−3325.

(11) Rifkin, S. C.; Evans, D. H. *J. Electrochem. Soc.* **1974**, *121*, 769−773.

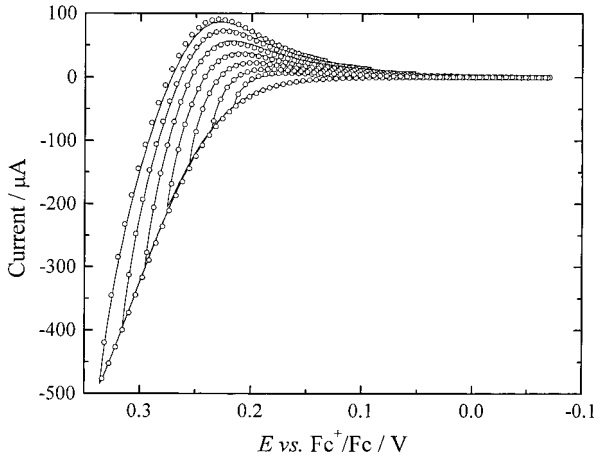

Figure 5. Cyclic voltammograms (full curves) with various switching potentials prior to the anodic peak. 10.5 mM **1** at 0.5 V/s. Symbols: Digital simulations with the same parameters as in Figure 2 except that 60 Ω of solution resistance was used.

Figure 5 is a composite of seven voltammograms recorded with switching potentials that were 80, 60, 40, 20, and 0 mV negative of the standard potential for the $\mathbf{1}^{+\bullet}/\mathbf{1}$ couple as well as 20 and 40 mV positive of the standard potential. The current at the last of these switching potentials is about 90% of the anodic peak current. A relatively high concentration (10.5 mM) was selected so as to enhance the importance of second-order reactions. Also included in Figure 5 are simulations with $k_1 = 0.6\ s^{-1}$ (as established from the results shown in Figures 2−4) and $k_2 = k_3 = 100\ M^{-1}\ s^{-1}$. The agreement is excellent. The simulations are relatively insensitive to the relative values of k_2 and k_3, so great weight should not be put on the numbers given here. What is clear is the fact that neither proton transfer/hydrogen atom abstraction reactions 1 and 2 (k_2) nor disproportionation reaction 3 (k_3) can alone account for the results. Specifically with $k_1 = 0.6\ s^{-1}$, $k_2 = 120\ M^{-1}\ s^{-1}$, and $k_3 = 0$ (no disproportionation), the agreement was distinctly poorer than that shown in Figure 5. Conversely, with only disproportionation as the second-order process ($k_1 = 0.6\ s^{-1}$, $k_2 = 0$ and $k_3 = 500\ M^{-1}\ s^{-1}$), very poor agreement was found at the three to four switching potentials closest to the foot of the peak.

We have tried to devise experiments to distinguish between proton-transfer reaction 1 and hydrogen atom abstraction reaction 2. If the reaction of the radical cation of **1** is best understood as a proton transfer from the radical cation to unreacted amine (reaction 1), a base stronger than **1** should be even more effective in causing decomposition of the radical cation. The difficult-to-oxidize and much stronger base tetrabutylammonium hydroxide was added to a 1.74 mM solution of **1** and voltammograms were recorded at 1 V/s. Addition of 1 equiv of base had no effect on the anodic peak and caused about a 50% decrease in the cathodic peak. Unfortunately, this result is not definitive, but it does suggest that bases are not particularly effective in destroying the radical cation.

To test the ability of the radical cation, $\mathbf{1}^{+\bullet}$, to abstract a hydrogen atom from the neutral amine, **1**, (reaction 2) it would be desirable to add a compound with an α-CH bond dissociation energy similar to that of **1**. Triethylamine was chosen for this purpose, though it will be argued later that its bond dissociation energy is significantly lower than that of **1**. It was found that the peak for reduction of the radical cation in a voltammogram obtained at 1 V/s was completely suppressed by addition of only a 1:3 mole ratio of triethylamine to **1**. At the same time, the height of the anodic peak for oxidation of **1** to the radical cation increased. These observations could mean that $\mathbf{1}^{+\bullet}$ is lost as it abstracts a hydrogen atom from triethylamine forming the diethylaminoethyl radical whose oxidation at the electrode (or by $\mathbf{1}^{+\bullet}$) accounts for the enhanced anodic current.

Once again, however, the result is ambiguous. The irreversible anodic peak potential for triethylamine is only about 0.1 V more positive than the standard potential for the $\mathbf{1}^{+\bullet}/\mathbf{1}$ couple. Thus, the disappearance of $\mathbf{1}^{+\bullet}$ and the enhanced anodic current could just as well be due to the electron-transfer-catalyzed oxidation of triethylamine as observed by Wiseman with ferrocene derivatives as catalysts.[12] In this scheme, $\mathbf{1}^{+\bullet}$ accepts an electron from triethylamine forming **1** (whose oxidation produces the enhanced anodic current) and the triethylamine radical cation whose subsequent rapid and irreversible reactions drive the catalytic cycle.

Discussion

The various species to be considered are drawn in Scheme 2 with shorthand notation based on the **AB** core in which a hydrogen atom attached to **A** is a hydrogen on the α-carbon and a hydrogen atom attached to **B** is bonded to the nitrogen atom. The representation of the radical cation ($\mathbf{HAB}^{+\bullet}$) is meant to denote the through-bond coupling mentioned in the Introduction. In particular, it should be noted that $\mathbf{AB}^+$ is not an immonium cation ($R_2N^+{=}CR'_2$ with a $^+N{=}C$ π bond), in contrast to most α-amino radical one-electron-oxidation products because the bicyclooctane framework twists the orbitals at nitrogen and carbon to 90°. AM1 UHF calculations get $\mathbf{AB}^+$ to be a triplet, with the radical center at carbon having zero overlap with the delocalized σ-conjugated diamine radical cation, which has very similar charges on the nitrogens (−0.041 and −0.028 for the nitrogen next to the radical-bearing carbon).

We will first discuss the nature of the first-order decay of $\mathbf{1}^{+\bullet}$ ($\mathbf{HAB}^{+\bullet}$). The solution-phase homolytic bond dissociation energy of $\mathbf{HABH}^+$ (N−H bond scission) has been estimated to be 91 kcal/mol in acetonitrile.[13] This means that $\mathbf{HAB}^{+\bullet}$ is a relatively good hydrogen atom acceptor and should be capable of abstracting hydrogen atoms from a number of donors in the solvent and electrolyte system. The bond dissociation energy of acetonitrile in the gas phase is 93 kcal/mol,[14] so the solvent, which is present in great excess, may possibly be the hydrogen atom source for the pseudo-first-order decay of $\mathbf{HAB}^{+\bullet}$ detected in this work, $k_1 = 0.6\ s^{-1}$. A second possibility as a hydrogen atom source is the tetrabutylammonium ion from the electrolyte.

We turn next to the relative energetics of the reactions of $\mathbf{HAB}^{+\bullet}$ as indicated in reactions 1−3. Reactions 1 and 2 share the same reactants and products, so the free energy changes of the reactions are identical ($\Delta G_1^\circ =$

(12) Wiseman, E. L. Master's Thesis, University of Texas at Austin, 1995.
(13) Liu, W.-Z.; Bordwell, F. G. *J. Org. Chem.* **1996**, *61*, 4778−4783.
(14) McMillen, D. F.; Golden, D. M. *Annu. Rev. Phys. Chem.* **1982**, *33*, 493−532.

$\Delta G_2^\circ = \Delta G_{1,2}^\circ$). Therefore, whether the reaction is a proton transfer (reaction 1) or a hydrogen atom transfer (reaction 2) is a function of the intrinsic barriers of the processes and not the driving forces, which are the same. The magnitude of the free energy change in acetonitrile is given by eq 4.

$$\Delta G_{1,2}^\circ = 2.303RT[\mathrm{p}K_a(\mathbf{HAB}^{+\bullet}) - \mathrm{p}K_a(\mathbf{HABH}^+)] \quad (4)$$

The value of $\mathrm{p}K_a(\mathbf{HABH}^+)$ in acetonitrile is[15] 18.3, but $\mathrm{p}K_a(\mathbf{HAB}^{+\bullet})$ is not available. However, an estimate can be obtained using the principles reviewed by Wayner and Parker.[16] Equation 5 provides a route to $\mathrm{p}K_a(\mathbf{HAB}^{+\bullet})$ from standard potentials and the solution-phase bond dissociation free energy of **HAB**, $\mathrm{BDFE}_{\mathrm{HAB}}$.

$$\mathrm{p}K_a(\mathbf{HAB}^{+\bullet}) = \frac{\mathrm{BDFE}_{\mathrm{HAB}}}{2.303RT} + \frac{E^\circ_{\mathrm{H}^+/\mathrm{H}\bullet} - E^\circ_{\mathrm{HAB}^{+\bullet}/\mathrm{HAB}}}{2.303RT/F} \quad (5)$$

Unfortunately, $\mathrm{BDFE}_{\mathrm{HAB}}$ is also unavailable, but an approximate result can be obtained by using the gas-phase bond dissociation energy, $\mathrm{BDE}_{\mathrm{HAB}}$, an enthalpy change. Experimental values are not available and a variety of results have been obtained for other tertiary amines, such as trimethylamine, where experimental values fall in the 84−89 kcal/mol range and theoretical values are near 92 kcal/mol.[17] In any case, the C−H bond dissociation energy of **1** (**HAB**) will be significantly larger than that for trimethylamine owing to a stereoelectronic effect that destabilizes the α-aminoalkyl radical from **1** compared to that of an acyclic amine. We estimate $\mathrm{BDE}_{\mathrm{HAB}\bullet}$ to be about 93 kcal/mol.[18]

The value of $E^\circ_{\mathrm{H}^+,\mathrm{H}^\bullet}$ for acetonitrile is[19] −1.77 V vs aqueous NHE or −2.41 V vs ferrocene in acetonitrile.[20] The standard potential for the $\mathbf{HAB}^{+\bullet}/\mathbf{HAB}$ couple measured in this work is +0.30 V vs ferrocene. Insertion of the above values in eq 4 gives $\mathrm{p}K_a(\mathbf{HAB}^{+\bullet}) = 22$, which must be regarded as approximate owing to the replacement of solution-phase $\mathrm{BDFE}_{\mathrm{HAB}}$ by an estimated gas-phase $\mathrm{BDE}_{\mathrm{HAB}}$, a process that neglects free energies of solvation and entropic effects. Putting $\mathrm{p}K_a(\mathbf{HAB}^{+\bullet}) = 22$ and $\mathrm{p}K_a(\mathbf{HABH}^+) = 18.3$ in eq 4 gives $\Delta G_{1,2}^\circ = 5$ kcal/mol; i.e., reactions 1 and 2 are predicted to be slightly uphill processes.

By contrast, hydrogen-atom-transfer disproportionation (reaction 3) is strongly favored with a large driving force. The free energy change for this reaction, ΔG_3°, can be obtained from the previously determined $\mathrm{p}K_a$ values and standard potentials through a thermodynamic cycle giving eq 6.

$$\Delta G_3^\circ = 2.303RT[\mathrm{p}K_a(\mathbf{HAB}^{+\bullet}) - \mathrm{p}K_a(\mathbf{HABH}^+)] + F(E^\circ_{\mathrm{AB}^+/\mathrm{AB}\bullet} - E^\circ_{\mathrm{HAB}^{+\bullet}/\mathrm{HAB}}) \quad (6)$$

We were unable to measure the standard potential for the **AB** cation/α-aminoalkyl radical couple, $E^\circ_{\mathrm{AB}^+/\mathrm{AB}^\bullet}$, but the values are known to be quite negative.[2,21] If we assume that the value is the same as that measured for the triethylamine system (−1.12 V vs aqueous SCE;[21] −1.52 V vs ferrocene in acetonitrile), it is predicted that $\Delta G_3^\circ = -37$ kcal/mol, i.e. hydrogen-atom-transfer disproportionation is strongly favored.[22]

Thus, we conclude that proton transfer and hydrogen atom transfer (reactions 1 and 2) are not favored though our results indicate that they proceed at a relatively slow but measurable rate. Hydrogen-atom-transfer disproortionation (reaction 3) is predicted to be favored by 37 kcal/mol, and the present results provide the first kinetic evidence for its occurrence though its rate constant is not significantly larger that those of reactions 1 and 2. One reason for the relatively small rate constant for disproportionation may be charge repulsion when the two radical cations approach one another.

Amine radical cations are able to abstract unactivated secondary C−H rapidly enough to carry chains in the Hofmann−Löffler−Freytag reaction.[23] It is likely that $\mathbf{1}^{+\bullet}$ is slightly more reactive in hydrogen atom abstraction reactions than an ordinary $R_3N^{+\bullet}$ because its nitrogen atoms are pyramidalized, reducing the geometry reorganization necessary for the reaction. Also, Parker et al.[24] have reported efficient hydrogen atom abstraction by the radical cations of 9-phenylacridine and derivatives.

Experimental Section

Instrumentation and Procedures. The electrochemical apparatus has been described previously.[25] The working electrode was either a platinum or gold disk (0.30 cm diameter). The laboratory reference electrode comprised a silver wire in contact with 0.010 M $AgNO_3$, 0.10 M Bu_4NPF_6 in acetonitrile. The standard potential for the ferrocenium ion/ferrocene couple was frequently measured with respect to the laboratory reference, and all potentials reported herein are with respect to the ferrocene potential. The experiments were conducted at room temperature.

(15) Coetzee, J. F.; Padmanabhan, G. R. *J. Am. Chem. Soc.* **1965**, *87*, 5005−5010.

(16) Wayner, D. D. M.; Parker, V. D. *Acc. Chem. Res.* **1993**, *26*, 287−294.

(17) (a) Griller, D.; Lossing, F. P. *J. Am. Chem. Soc.* **1981**, *103*, 1586−1587. (b) Clark, K. B.; Wayner, D. D. M.; Demirdji, S. H.; Koch, T. H. *J. Am. Chem. Soc.* **1993**, *115*, 2447−2453. (c) Wayner, D. D. M.; Clark, K. B.; Rauk, A.; Yu, D.; Armstrong, D. A. *J. Am. Chem. Soc.* **1997**, *119*, 8925−8932. (d) Dombrowski, G. W.; Dinnocenzo, J. P.; Farid, S.; Goodman, J. L.; Gould, I. R. *J. Org. Chem.* **1999**, *64*, 427−431.

(18) (a) In the radical formed by removal of a hydrogen atom from **1**, there is poor overlap between the spin-bearing orbital on carbon and the lone pair orbital on nitrogen owing to geometric constraints imposed by the bicyclic system (see depiction of $\mathbf{AB}^\bullet$ in Scheme 2). Acyclic α-aminoalkyl radicals are stabilized by a three-electron π-bonding interaction,[18b] a stabilization not available to $\mathbf{AB}^\bullet$. AM1 UHV calculations of absolute bond dissociation energies are not accurate, but relative values are more accurately predicted. For example, AM1 predicts that the value for triethylamine is 8 kcal/mol greater than that for triallylamine, in exact agreement with experiment.[17d] Similar calculations for **1** vs trimethylamine indicate the bond dissociation energy for the former to be 6 kcal/mol greater than the latter. Taking an average experimental value for trimethylamine of 87 kcal/mol[17] gives an estimate of 93 kcal/mol for $\mathrm{BDE}_{\mathrm{HAB}}$. (b) Griller, D.; Howard, J. A.; Marriott, P. R.; Scaiano, J. C. *J. Am. Chem. Soc.* **1981**, *103*, 619−623.

(19) Parker, V. D. *J. Am. Chem. Soc.* **1992**, *114*, 7458−7462.

(20) Shalev, H.; Evans, D. H. *J. Am. Chem. Soc.* **1989**, *111*, 2667−2674.

(21) Wayner, D. D. M.; McPhee, D. J.; Griller, D. *J. Am. Chem. Soc.* **1988**, *110*, 132−137.

(22) It might be argued that the standard potential for the $\mathbf{AB}^+/\mathbf{AB}^\bullet$ couple might be pushed in the negative direction by the destabilization of the radical.[18] However, as discussed above, the cation will also be destabilized owing to poor overlap of the C_α p-orbital with the adjacent lone pair orbital destroying the π-bonding interaction present in typical immonium ions. Thus, using the experimental value for triethylamine appears to be reasonable.

(23) (a) Wolff, M. E. *Chem. Rev.* **1963**, *63*, 55−64. (b) Schmittel, M.; Burghart, A. *Angew. Chem., Int. Ed. Engl.* **1997**, *36*, 2550−2589.

(24) Handoo, K. L.; Cheng, J.-P.; Parker, V. D. *Acta Chem. Scand.* **1993**, *47*, 626−628.

(25) Oliver, E. W.; Evans, D. H.; Caspar, J. V *J. Electroanal. Chem.* **1996**, *403*, 153−158.

Electronic resistance compensation was applied to correct for about two-thirds of the IR drop. The remaining resistance was included in the simulation program used for data analysis.

Digital simulations were performed with the software package DigiSim (Bioanalytical Systems, version 2.1). Planar diffusion geometry was used, and the size of each potential step was 1 mV.

Chemicals. Optima-grade acetonitrile (Fisher) was used as received. The electrolytes (0.10 M) were either tetrabutylammonium perchlorate or lithium perchlorate and were purified according to standard methods. The electrolyte solution was passed through a column of activated alumina before each experiment. 1,4-Diazabicyclo[2.2.2]-octane was used as received from Fisher.

Preparative Experiments. The controlled potential electrolyses were carried out in a glass cell with a platinum gauze working electrode (ca. 10 cm^2 geometric area). The auxiliary electrode compartment was separated from the working electrode compartment by a layer of hard-surface paper (Keuffel and Esser Albanene tracing paper). The charge passed to completely remove **1** was typically 0.8 faraday/mol. After electrolysis, the acetonitrile was evaporated and the residue washed with acetone. After evaporation of acetone, the residue was recrystallized from ethanol giving the hydroperchlorate of **1**, $C_6H_{12}N_2 \cdot HClO_4$, in 70% yield. ^1H NMR δ 3.09 ppm (s, 12 H). mp 230 °C (dec.).

Acknowledgment. This work was supported by the National Science Foundation, Grant CHE-9704211 (D.H.E.) and in part by Grant CHE-9417546 (S.F.N.). We also thank Stephen E. Treimer for preliminary experiments.

JO991709V